Inorg. Chem. **2007**, *46*, 11235–11242

Azide-Bridged One-Dimensional Mn^{III} Polymers: Effects of Side Group of Schiff Base Ligands on Structure and Magnetism

Mei Yuan,[†,‡] Fei Zhao,[†] Wen Zhang,[†] Zhe-Ming Wang,[†] and Song Gao*[,†]

Beijing National Laboratory for Molecular Sciences, State Key Laboratory of Rare Earth Materials Chemistry and Applications, College of Chemistry and Molecular Engineering, Peking University, Beijing 100871, People's Republic of China and Technical Institute of Physics and Chemistry, Chinese Academy of Sciences, Beijing 100080, People's Republic of China

Received August 22, 2007

By changing ancillary tetradentate Schiff base ligands (L), two new one-dimensional azide-bridged manganese(III) coordination complexes $[Mn^{III}(L)(\mu_{1,3}\text{-}N_3)]_n$ [L = 5-Fsalen (**1**), 5-OCH_3 (**2**); salen = *N*,*N*′-bis(salicylidene)-1,2-diaminoethane] as well as a mononuclear complex $[Mn^{III}(salophen)(N_3)]$ (**3**) [salophen = *N*,*N*′-bis(salicylidene)-*o*-phenylenediamine] have been successfully obtained. All of them have been structurally and magnetically characterized. In the structures of **1**–**3** each Mn^{III} ion is in a distorted octahedral geometry with an obvious Jahn–Teller effect, where the tetradentate L ligands all bind in the equatorial mode, whereas in the axial direction, the N_3^- ion acts as an end-to-end bridge in **1** and **2** while a terminal group in **3** with a methanol molecule at the other end. Magnetic characterization shows that the $\mu_{1,3}$-bridging azide ion proves to mainly transmit antiferromagnetic interaction between Mn^{III} ions, but these three complexes exhibit various magnetic behaviors at low temperatures. Noteworthily, complex **2** behaves as a weak ferromagnet with a relatively large coercive field of 2.3 kOe, much larger than the value reported previously.

Introduction

The design and synthesis of transition-metal coordination polymers bridged by small conjugated ligands, such as cyano, azido, oxalato, thiocyano, and nitrido, are currently under intense investigation in view of their structure diversity and in the context of molecule-based magnets.[1] Among these short bridging ligands, in particular, the azide ion exhibits versatile bridging modes, such as μ-(1,3),[2] μ-(1,1),[3] and rare μ-(1,1,3),[4] the latter two modes of which usually transfer ferromagnetic interactions between metal centers. To date, plenty of studies about the azide bridge have been dedicated to some divalent transition-metal coordination complexes (Cu^{2+}, Co^{2+}, Ni^{2+}, Fe^{2+}, Mn^{2+}, etc.), possessing diverse structures from 1-D, 2-D, to 3-D supramolecular polymers with various magnetic properties.[5−7] On the other hand, the Mn^{III} ion itself has a high spin number and an obvious single-ion anisotropy, leading to intriguing molecule-based magnets,

* To whom correspondence should be addressed. E-mail: gaosong@pku.edu.cn.
† Peking University.
‡ Chinese Academy of Sciences.

(1) (a) Ferlay, S.; Mallah, T.; Ouahes, R.; Veillet, P.; Verdaguer, M. *Nature* **1995**, *378*, 701. (b) Sato, O.; Iyoda, T.; Fujishima, A.; Hashimoto, K. *Science* **1996**, *272*, 704. (c) Tamaki, H.; Zhong, Z. J.; Matsumoto, N.; Kida, S.; Koikawa, K.; Achiwa, N.; Okawa, H. *J. Am. Chem. Soc.* **1992**, *114*, 6974. (d) Ribas, J.; Escuer, A.; Monfort, M.; Vicente, R.; Cortes, R.; Lezama, L.; Rojo, T. *Coord. Chem. Rev.* **1999**, *193*, 1027 and references therein. (e) Ma, B. Q.; Gao, S.; Su, G.; Xu, G. X. *Angew. Chem., Int. Ed.* **2001**, *40*, 434. (f) Larionova, J.; Sanchiz, J.; Gohlen, S.; Ouahab, L.; Kahn, O. *Chem. Commun.* **1998**, 953. (g) Yuan, M.; Zhao, F.; Zhang, W.; Pan, F.; Wang, Z. M.; Gao, S. *Chem. Eur. J.* **2007**, *13*, 2937.

(2) (a) Ribas, J.; Monfort, M.; Ghosh, B. K.; Cortes, R.; Solans, X.; Font-Bardia, M. *Inorg. Chem.* **1996**, *35*, 864. (b) Tuczek, F.; Bensch, W. *Inorg. Chem.* **1995**, *34*, 1482. (c) Escuer, A.; Vicente, R.; Goher, M. A. S.; Mautner, F. A. *Inorg. Chem.* **1995**, *34*, 5707. (d) Stults, B. R.; Marianelli, R. S.; Day, V. W. *Inorg. Chem.* **1975**, *14*, 722.

(3) (a) Ribas, J.; Monfort, M.; Diaz, C.; Bastos, C.; Solans, X. *Inorg. Chem.* **1994**, *33*, 484. (b) Mautner, A. F.; Goher, M. A. S. *Polyhedron* **1996**, *15*, 1133. (c) Cortes, R.; Pizarro, J. L.; Lezama, L.; Arriortua, M. I.; Rojo, T. *Inorg. Chem.* **1994**, *33*, 2697. (d) De Munno, D.; Poerio, T.; Viau, G.; Julve, M.; Lloret, F. *Angew. Chem., Int. Ed. Engl.* **1997**, *36*, 1459.

(4) Wemple, M. W.; Adams, D. M.; Hagen, K. S.; Folting, K.; Hendrickson, D. N.; Christou, G. *J. Chem. Soc., Chem. Commun.* **1995**, 1591.

(5) (a) Monfort, M.; Resino, I.; Ribas, J.; Stoeckli-Evans, H. *Angew. Chem., Int. Ed.* **2000**, *39*, 191. (b) Escuer, A.; Vicente, R.; Goher, M. A. S.; Mautner, F. A. *Inorg. Chem.* **1997**, *36*, 3440. (c) Goher, M. A. S.; Cano, J.; Journaux, Y.; Abu-Youssef, M. A. M.; Mautner, F. A.; Escuer, A.; Vicente, R. *Chem. Eur. J.* **2000**, *6*, 778. (d) Mautner, F. A.; Cortés, R.; Lezama, L.; Rojo, T. *Angew. Chem., Int. Ed. Engl.* **1996**, *35*, 78. (e) Escuer, A.; Vicente, R.; Mautner, F. A.; Goher, M. A. S. *Inorg. Chem.* **1997**, *36*, 1233. (f) Liu, X. T.; Wang, X. Y.; Zhang, W. X.; Cui, P.; Gao, S. *Adv. Mater.* **2006**, *18*, 2852. (g) Das, A.; Rosair, G. M.; El Fallah, M. S.; Ribas, J.; Mitra, S. *Inorg. Chem.* **2006**, *45*, 3301.

10.1021/ic701655w CCC: $37.00
Published on Web 11/22/2007

especially for Mn^{III}-containing single-molecule magnets or single-chain magnets.[8] Also, manganese(III) coordination complexes were found to play important roles in the catalyst and biological field.[9] However, trivalent manganese(III)-based coordination polymers bridged by the azide ion have been rarely reported.[10−12]

According to the literature on manganese(III), tetradentate Schiff bases (SBs) proved to be effective auxiliary ligands to stabilize the high oxidation state of manganese but usually led to low-dimensional Mn^{III} compounds. Among those azide-bridged Mn^{III} chains, $[Mn(SB)(N_3)]_n$, the azide bridge is inclined to adopt an end-to-end μ-(1,3) mode and pass antiferromagnetic interaction.[10,11] Recently, another interesting azide-bridged Mn^{III} complex, $[Mn(5\text{-}Brsalen)(N_3)]_n$, was reported with coexistence of spin canting and metamagnetism.[12] Herein, by changing the side group of SB ligands, we obtained two new azide-bridged one-dimensional manganese(III) polymers, $[Mn^{III}(L)(\mu_{1,3}\text{-}N_3)]_n$ [L = 5-Fsalen (**1**), 5-OCH_3 (**2**); salen = *N*,*N*′-bis(salicylidene)-1,2-diaminoethane], as well as a mononuclear complex, $[Mn^{III}(salophen)(N_3)]$ (**3**) [salophen = *N*,*N*′-bis(salicylidene)-*o*-phenylenediamine], linked through extensive hydrogen-bond interactions into a two-dimensional supramolecular network. Magnetic studies show that these three complexes exhibit various magnetic behaviors at low temperatures. It is noteworthy that complex **2** behaves as a weak ferromagnet with a relatively large coercive field of 2.3 kOe, more than 10 times of that of the reported complex $[Mn(5\text{-}Brsalen)(N_3)]_n$, although they have very similar structures except for the side group of SBs.

Experimental Section

General Procedure. All starting materials were commercially available, reagent grade, and used as purchased without further purification. The quadridentate Schiff base ligands H_2L were synthesized by mixing the corresponding salicylaldehyde and diamine in a 2:1 mole ratio in ethanol according to the literature.[13]

CAUTION! Perchlorate salts of metal complexes with organic ligands are potentially explosive. Only small quantities of these complexes should be prepared and handled with proper protection.

$[Mn^{III}(L)(H_2O)]ClO_4$. The corresponding manganese(III)−SB precursors were obtained by mixing manganese(III) acetate dihydrate (1.00 g, 3.73 mmol) and H_2L (3.73 mmol) in methanol (200 mL) and anhydrous sodium perchlorate (0.69 g, 5.64 mmol) in water (80 mL). After evaporation to 40 mL and cooling, the resulting black crystals were collected by suction filtration.[14]

$[Mn^{III}(5\text{-}Fsalen)(\mu_{1,3}\text{-}N_3)]_n$ (1). Complex **1** was prepared by slow diffusion of concentrated methanolic solutions of NaN_3 (0.013 g, 0.2 mmol) and $[Mn(5\text{-}Fsalen)(H_2O)]ClO_4$ (0.0712 g, 0.15 mmol) in the two arms of an H tube, respectively. After about 2 weeks, red needle crystals of **1** were formed with a 70% yield. IR (KBr): $\nu(N_3)$ 2025(s), 1988(w); ν(CH=N) 1632(s). Anal. Calcd for $C_{16}H_{12}F_2MnN_5O_2$: C, 48.14; H, 3.03; N, 17.54. Found: C, 48.15; H, 3.10; N, 17.93.

$[Mn^{III}(5\text{-}OCH_3salen)(\mu_{1,3}\text{-}N_3)]_n$ (2). The preparation of **2** was analogous to that described for **1** except for H_2-5OCH_3salen instead of H_2-5Fsalen. Yield: 70%. IR (KBr): $\nu(N_3)$ 2026(s), 1987(w); ν(CH=N) 1624(m). Anal. Calcd for $C_{18}H_{18}MnN_5O_4$: C, 51.07; H, 4.29; N, 16.54. Found: C, 50.96; H, 4.33; N, 16.47.

$[Mn^{III}(salophen)(N_3)(H_2O)]$ (3). A similar preparation to that presented for **1** was used for **3** using H_2salophen instead of H_2-5Fsalen. A big block of deep brown crystals was collected. Yield: 80%.$\nu(N_3)$ 2044(s); ν(CH=N) 1605(s). Anal. Calcd for $C_{21}H_{18}MnN_5O_3$: C, 56.89; H, 4.09; N, 15.80. Found: C, 56.98; H, 4.22; N, 16.27.

Physical Measurements. Elemental analyses of carbon, hydrogen, and nitrogen were carried out with an Elementar Vario EL. The microinfrared spectroscopy studies were performed on a Magna-IR 750 spectrophotometer in the 4000−500 cm^{-1} region.

Magnetic Measurements. Variable-temperature magnetic susceptibility, zero-field ac magnetic susceptibility measurements, and field dependence of magnetization were performed on an Oxford Maglab 2000 System or Quantum Design MPMS-XL5 SQUID magnetometer. The experimental susceptibilities were corrected for the diamagnetism of the constituent atoms (Pascal's tables).

X-ray Crystallography. Data collections of all complexes were made on a NONIUS Kappa-CCD with Mo Kα radiation (λ = 0.71073 Å) at 293 K. The structures were solved by direct methods using the program SHELXS-97 and refined by a full-matrix least-squares technique based on F^2 using the SHELXL 97 program.[15] All of the non-hydrogen atoms were refined anisotropically. Hydrogen atoms defined by the stereochemistry were placed at their calculated positions and allowed to ride onto their host carbons in

(6) (a) Ribas, J.; Monfort, M.; Costa, R.; Solans, X. *Inorg. Chem.* **1993**, *32*, 695. (b) Manson, J. L.; Arif, A. M.; Miller, J. S. *Chem. Commun.* **1999**, 1479. (c) Hao, X.; Wei, Y.; Zhang, S. W. *Chem. Commun.* **2000**, 2271.

(7) (a) Ma, B. Q.; Sun, H. L.; Gao, S.; Su, G. *Chem. Mater.* **2001**, *13*, 1946. (b) Gao, E. Q.; Wang, Z. M.; Yan, C. H. *Chem. Commun.* **2003**, 1748. (c) Chen, H. J.; Mao, Z. W.; Gao, S.; Chen, X. M. *Chem. Commun.* **2001**, 2320.

(8) (a) Tasiopoulos, A. J.; Vinslava, A.; Wernsdorfer, W.; Abboud, K. A.; Christou, G. *Angew. Chem. Int. Ed.* **2004**, *43*, 2117. (b) Sañudo, E. C.; Wernsdorfer, W.; Abboud, K. A.; Christou, G. *Inorg. Chem.* **2004**, *43*, 4137. (c) Murugesu, M.; Habrych, M.; Wernsdorfer, W.; Abboud, K. A.; Christou, G. *J. Am. Chem. Soc.* **2004**, *126*, 4766. (d) Murugesu, M.; Raftery, J.; Wernsdorfer, W.; Christou, G.; Brechin, E. K. *Inorg. Chem.* **2004**, *43*, 4203. (e) Miyasaka, H.; Clérac, R.; Wernsdorfer, W.; Lecren, L.; Bonhomme, C.; Sugiura, K.-i.; Yamashita, M. *Angew. Chem., Int. Ed.* **2004**, *43*, 2801. (f) Escuer, A.; Aromí, G. *Eur. J. Inorg. Chem.* **2006**, 4721. (g) Milios, C. J.; Vinslava, A.; Wood, P. A.; Parsons, S.; Wernsdorfer, W.; Christou, G.; Perlepes, S. P.; Brechin, E. K. *J. Am. Chem. Soc.* **2007**, *129*, 8. (h) Mereacre, V. M.; Ako, A. M.; Clerac, R.; Wernsdorfer, W.; Filoti, G.; Bartolome, J.; Anson, C. E.; Powell, A. K. *J. Am. Chem. Soc.* **2007**, *129*, 9248.

(9) (a) Ludwig, M. L.; Pattridge, K. A.; Stallings, W. C. *Manganese in Metabolism and Enzyme Function*; Academic Press: New York, 1986; Chapter 21, p 405. (b) Beyer, W. F., Jr.; Fridovich, I. *Manganese in Metabolism and Enzyme Function*; Academic Press: New York, 1986; Chapter 12, p 193. (c) Pecoraro, V. L. *Photochem. Photobiol.* **1986**, *48*, 249.

(10) (a) Reddy, K. R.; Rajasekharan, M. V.; Tuchagues, J. P. *Inorg. Chem.* **1998**, *37*, 5978. (b) Li, H.; Zhong, Z. J.; Duan, C. Y.; Yu, X. Z.; Mak, T. C. W.; Wu, B. *Inorg. Chim. Acta* **1998**, *271*, 99.

(11) (a) Panja, A.; Shaikh, N.; Vojtíšek, P.; Gao, S.; Banerjee, P. *New J. Chem.* **2002**, *26*, 1025. (b) Kennedy, B. J.; Murray, K. S. *Inorg. Chem.* **1985**, *24*, 1552.

(12) Ko, H. H.; Lim, J. H.; Kim, H. C.; Hong, C. S. *Inorg. Chem.* **2006**, *45*, 8847.

(13) (a) Aurangzeb, N.; Hulme, C. E.; McAuliffe, C. A.; Pritchard, R. G.; Watkinson, M.; Garcia-Deibe, A.; Bermejo, M. R.; Sousa, A. *J. Chem. Soc., Chem. Commun.* **1992**, 1524. (b) Aurangzeb, N.; Hulme, C. E.; McAuliffe, C. A.; Pritchard, R. G.; Watkinson, M.; Bermejo, M. R.; Sousa, A. *J. Chem. Soc., Chem. Commun.* **1994**, 2193.

(14) Przychodzeń, P.; Lewiński, K.; Balanda, M.; Pelka, R.; Rams, M.; Wasiutyński, T.; Duhayon, C. G.; Sieklucka, B. *Inorg. Chem.* **2004**, *43*, 2967.

(15) (a) Sheldrick, G. M. *SHELXL 97, Program for Crystal Structure Refinement*; University of Göttingen: Göttingen, Germany, 1998. (b) Sheldrick, G. M. SHELXS 97, Program for Crystal Structure Solution. *Acta Crsystallogr., Sect. A* **1990**, *46*, 467.

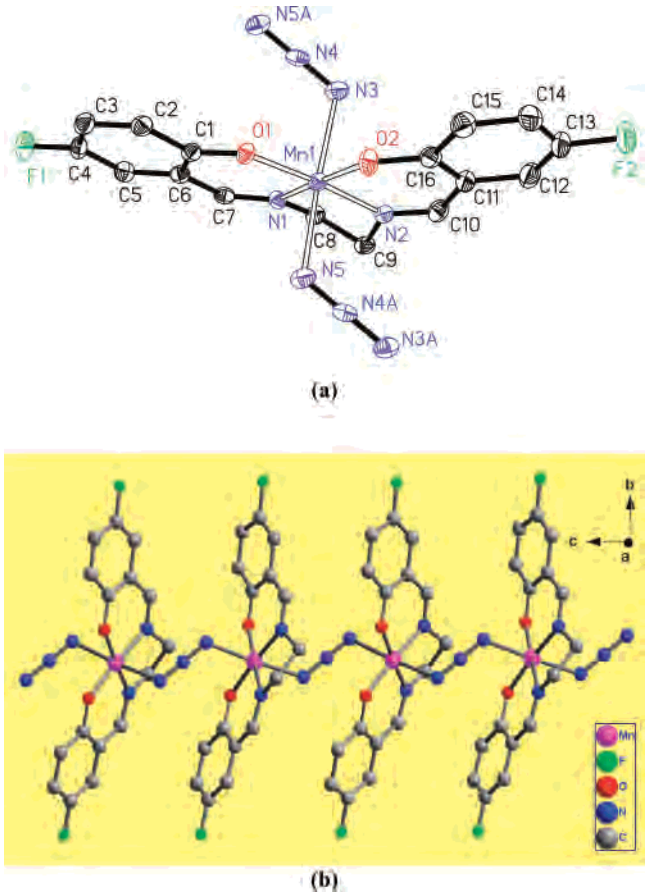

Figure 1. (a) ORTEP drawing with the atom-labeling scheme of **1** (30% probability ellipsoids). (b) View of the one-dimensional zigzag chain of **1**.

Table 1. Crystallographic Information for Complexes **1**−**3**

	1	**2**	**3**
formula	$C_{16}H_{12}F_2MnN_5O_2$	$C_{18}H_{18}MnN_5O_4$	$C_{21}H_{18}MnN_5O_3$
fw	399.25	423.31	443.34
cryst syst	orthorhombic	orthorhombic	triclinic
space group	$Pca2_1$	$Pbca$	$P\bar{1}$
a (Å)	10.804(2)	10.862(2)	7.9707(16)
b (Å)	13.453(3)	11.184(2)	10.064(2)
c (Å)	11.166(2)	29.688(6)	12.057(2)
α (deg)	90	90	97.65(3)
β (deg)	90	90	91.31(3)
γ (deg)	90	90	91.85(3)
V (Å^3)	1622.9(6)	3606.5(12)	957.7(3)
Z	4	8	2
d_{calc} (g cm^{-3})	1.634	1.559	1.537
μ (mm^{-1})	0.857	0.769	0.724
F(000)	808	1744	456
reflns collected	27 377	35 336	18 083
unique reflns	3703	4075	4355
GoF	1.012	1.013	0.990
R1[a]	0.0352	0.0455	0.0417
wR2[b]	0.0626	0.0616	0.0808

[a] $R_1 = \Sigma||F_o| - |F_c||/\Sigma|F_o|$. [b] $wR_2 = \Sigma[w(F_o^2 - F_c^2)^2]/\Sigma[w(F_o^2)^2]^{1/2}$.

coordinates. The details of the crystallographic data are listed in Table 1, and selected bond lengths and angles are listed in Table 2.

Results and Discussion

FTIR Spectra. In the IR spectra complexes **1**−**3** all exhibit strong absorption in a range of 2020−2060 cm^{-1}, assignable to the asymmetric stretching vibration of the N_3 moiety in which the presence of weak splitting peaks below 2000 cm^{-1} confirms the bridging coordination mode of the N_3^- ligand in complexes **1** and **2** while the absence of a splitting peak proves the terminal mode of the N_3^- ligand in complex **1**. Also, the strong characteristic absorption of the CH═N group is also detected in the range of 1600−1700 cm^{-1}.

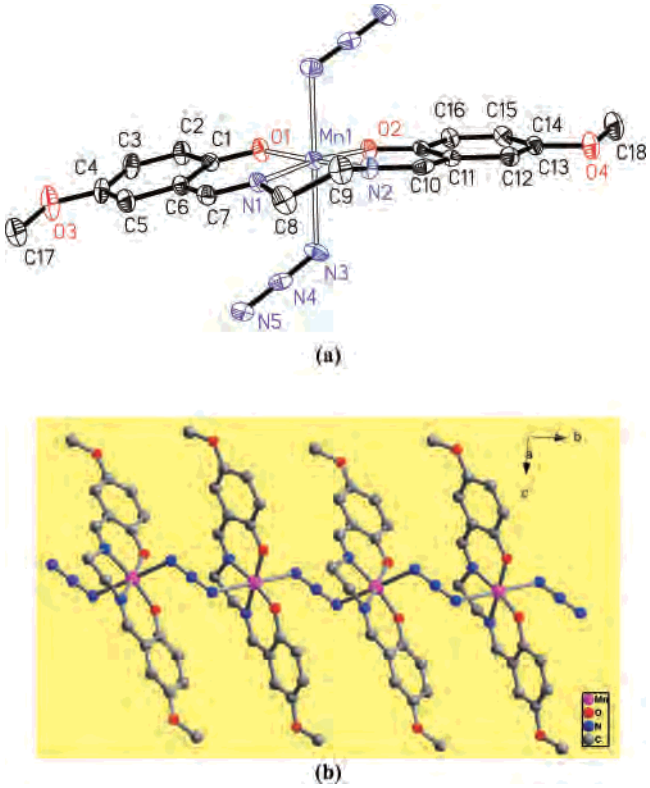

Figure 2. (a) ORTEP drawing with the atom-labeling scheme of **2** (30% probability ellipsoids). (b) View of the one-dimensional zigzag chain of **2**.

Crystal Structures of Complexes 1−3. Single-crystal X-ray analyses reveal that complexes **1** and **2** both consist of one-dimensional chains based on [Mn^{III}(L)] subunits except for the side group of the Schiff base ligand. The ORTEP plot of complex **1** is shown in Figure 1a. There is only one crystallographically independent manganese(III) atom in a distorted octahedral geometry, which is coordinated by the N_2O_2 donor atoms from one 5-Fsalen ligand in the equatorial mode and two N donor atoms from two N_3^- ions in the axial position. Each azide ligand functions as a trans-$\mu_{1,3}$ bridge to link monomeric [Mn^{III}(5-Fsalen)]$^+$ units into a one-dimensional ziazag chain along the c axis (Figure 1b), which belongs to Type I azide-bridged chain according to Prof. Escuer's classified method.[16] In the equatorial plane the bond lengths of Mn(1)−O(1), Mn(1)−O(2), Mn(1)−N(1), and Mn(1)−N(2) are 1.875(2), 1.883(2), 1.976(2), and 1.986(2) Å, respectively, which are close to those in other Mn^{III}−salen complexes.[11,12] The O(1) and N(2) atoms are below the equatorial plane at 0.034 and 0.037 Å, the O(2) and N(1) atoms are above at 0.040 and 0.041 Å, and the centered Mn^{III} ion is only above the plane at 0.01 Å. In comparison with the reported compound, [Mn(salen)N_3], in

(16) Escuer, R.; Vicente, R.; Fallah, M. S. E.; Ribas, J.; Solans, X. J. *J. Chem. Soc., Dalton Trans.* **1993**, 2973.

Table 2. Selected Bond Distances (Å) and Angles (deg) of Complexes **1**−**3**

		1[a]			
Mn(1)−O(1)	1.8751(18)	O(1)−Mn(1)−N(2)	173.60(10)	O(1)−Mn(1)−N(3)	91.45(10)
Mn(1)−O(2)	1.8834(18)	O(2)−Mn(1)−N(2)	91.80(9)	O(2)−Mn(1)−N(3)	89.54(9)
Mn(1)−N(2)	1.976(2)	O(1)−Mn(1)−N(1)	91.68(8)	N(2)−Mn(1)−N(3)	90.01(10)
Mn(1)−N(1)	1.986(2)	O(2)−Mn(1)−N(1)	173.24(8)	N(1)−Mn(1)−N(3)	87.43(9)
Mn(1)−N(5)	2.287(3)	N(2)−Mn(1)−N(1)	82.16(9)	N(5)−Mn(1)−N(3)	176.77(11)
Mn(1)−N(3)	2.327(3)	O(1)−Mn(1)−N(5)	91.76(10)	N(4)−N(3)−Mn(1)	114.7(2)
N(3)−N(4)	1.185(4)	O(2)−Mn(1)−N(5)	89.89(10)	N(3)−N(4)−N(5)#1	179.8(3)
N(4)−N(5)#1	1.186(4)	N(2)−Mn(1)−N(5)	86.84(10)	N(4)#2−N(5)−Mn(1)	118.5(2)
O(1)−Mn(1)−O(2)	94.44(8)	N(1)−Mn(1)−N(5)	92.79(9)		
		2[b]			
Mn(1)−O(2)	1.8677(19)	O(2)−Mn(1)−N(1)	172.05(10)	O(2)−Mn(1)−N(3)	89.91(9)
Mn(1)−O(1)	1.881(2)	O(1)−Mn(1)−N(1)	92.06(10)	O(1)−Mn(1)−N(3)	91.05(9)
Mn(1)−N(1)	1.974(2)	O(2)−Mn(1)−N(2)	91.96(10)	N(1)−Mn(1)−N(3)	84.40(10)
Mn(1)−N(2)	1.979(2)	O(1)−Mn(1)−N(2)	173.24(10)	N(2)−Mn(1)−N(3)	92.81(10)
Mn(1)−N(5)#1	2.300(3)	N(1)−Mn(1)−N(2)	82.81(11)	N(5)#1−Mn(1)−N(3)	178.03(10)
Mn(1)−N(3)	2.324(3)	O(2)−Mn(1)−N(5)#1	91.59(9)	N(4)−N(3)−Mn(1)	120.3(2)
N(3)−N(4)	1.179(3)	O(1)−Mn(1)−N(5)#1	90.12(9)	N(3)−N(4)−N(5)	178.3(3)
N(4)−N(5)	1.205(3)	N(1)−Mn(1)−N(5)#1	93.98(10)	N(4)−N(5)−Mn(1)#2	116.5(2)
O(2)−Mn(1)−O(1)	93.59(9)	N(2)−Mn(1)−N(5)#1	85.87(9)		
		3			
Mn(1)−O(1)	1.8642(16)	O(1)−Mn(1)−N(1)	92.14(7)	O(1)−Mn(1)−O(3)	88.81(7)
Mn(1)−O(2)	1.8923(15)	O(2)−Mn(1)−N(1)	170.81(7)	O(2)−Mn(1)−O(3)	88.03(7)
Mn(1)−N(1)	1.9896(18)	O(1)−Mn(1)−N(2)	173.06(7)	N(1)−Mn(1)−O(3)	84.63(7)
Mn(1)−N(2)	1.9964(18)	O(2)−Mn(1)−N(2)	92.38(7)	N(2)−Mn(1)−O(3)	87.33(7)
Mn(1)−N(3)	2.216(2)	N(1)−Mn(1)−N(2)	81.77(7)	N(3)−Mn(1)−O(3)	174.39(7)
Mn(1)−O(3)	2.3577(17)	O(1)−Mn(1)−N(3)	96.04(8)	N(4)−N(3)−Mn(1)	121.57(15)
N(3)−N(4)	1.180(3)	O(2)−Mn(1)−N(3)	94.50(7)	N(5)−N(4)−N(3)	177.9(3)
N(4)−N(5)	1.164(3)	N(1)−Mn(1)−N(3)	92.34(8)		
O(1)−Mn(1)−O(2)	93.24(7)	N(2)−Mn(1)−N(3)	87.56(8)		

[a] #1 $-x + 1/2, y, z + 1/2$. #2 $-x + 1/2, y, z - 1/2$. [b] #1 $-x + 1/2, y + 1/2, z$. #2 $-x + 1/2, y - 1/2, z$.

complex **1** Mn(1), O(1), O(2), N(1), and N(2) are more coplanar. As expected, the bond lengths in the axial position of Mn(1)−N(3) and Mn(1)−N(5) (2.287(3) and 2.327(3) Å) are elongated due to a Jahn−Teller distortion at the high-spin d^4 metal center;[10−12] the bond angles of Mn(1)−N(3)−N(4) and Mn(1)−N(5)−N(4A) are 114.7(2)° and 118.5(2)°, respectively. These values are also similar to those in [Mn(salen)N_3]. As for N_3^- itself, N(3)−N(4) and N(4)−N(5A) have almost the same bond lengths (1.185(4) and 1.186(4) Å) and the N(3)−N(4)−N(5A) bond angle is 179.8(3)°, close to 180°, obviously different from the asymmetric $NCNH^-$ bridge in the similar Mn^{III} polymers.[1g]

The space packing of complex **1** along the *b* axis is shown in Figure S1 (Supporting Information) in which hydrogen bonds link the azide-bridged chains into a three-dimensional supramolecular aggregation. The hydrogen bonds are mainly formed between C(8) and F(2) ($0.5 + x$, $2 - y$, z) and between C(5) and O(2) ($0.5 + x$, $1 - y$, z); the C(8)−H···F(2) and C(5)−H···O(2) distances are 3.153 and 3.485 Å, respectively, with corresponding angles of 131.4° and 166.5°. The shortest intrachain Mn···Mn distance is 5.583 Å compared to that in [Mn(salen)N_3] (5.56 Å), while the nearest interchain Mn···Mn distance is 7.130 Å, much shorter than that in [Mn(salen)N_3] (9.99 Å).[11]

In the structure of complex **2** (Figure 2a) the Schiff base ligand 5-OCH_3salen^{2-} replaces the 5-Fsalen^{2-} and the one-dimensional azide-bridged chain is along the *b* axis (Figure 2b), different from complex **1**. The bond lengths of Mn(1)−N(3) and Mn(1)−N(5A) are 2.324(3) and 2.300(3) Å, respectively; the corresponding bond angles of Mn(1)−N(3)−N(4) and Mn(1A)−N(4)−N(5) are 120.3(2)° and 116.5(2)°. As shown in Figure S2 (Supporting Information), plenty of hydrogen bonds also exist in the crystal packing of complex **2**, which are mainly between C(2) and O(4) ($0.5 + x$, y, $0.5 - z$) with a C(2)···O(4) distance of 3.440 Å and corresponding angle of 156.8°. The shortest intrachain Mn···Mn distance is 5.592 Å, close to that in **1**, whereas the nearest interchain Mn···Mn distance is 7.219 Å, a little longer than that in **1**.

Different from the one-dimensional azide-bridged chains of complexes **1** and **2**, complex **3** is only a mononuclear structure, which may be caused by the steric effect of the rigid Schiff base ligangd H_2-salophen, preventing formation of an infinite chain. As shown in Figure 3a, in the equatorial plane each Mn^{III} center coordinates to O(1), N(1), N(2), and O(2) from one salophen^{2-} ligand; the bond lengths of Mn(1)−O(1), Mn(1)−O(2), Mn(1)−N(1), and Mn(1)−N(2) are 1.864(2), 1.892(2), 1.990(2), and 1.892(2) Å, respectively. In the apical position the Mn^{III} center is coordinated by one N_3^- ion and one methanol molecule as terminal ligands, respectively, finishing its distorted octahedral coordination atmosphere. As expected, the bond distances in the axial position (Mn(1)−N(3) 2.216(2) Å; Mn(1)−O(3) 2.358(2) Å) are significantly longer than those associated with the salophen^{2-} ligand due to a Jahn−Teller distortion of the Mn^{III} ion. The Mn(1)−N(3) length is a little longer than that in complexes **1** and **2** for the azide ion acts as a terminal ligand in **3** while a bridging ligand in **1** and **2**. In the crystal packing of complex **3** (Figure 3b) there are strong hydrogen-bonding contacts between O(3) from the coordinated methanol molecule and N(5) from the terminal N_3^- ion with an O(3)·

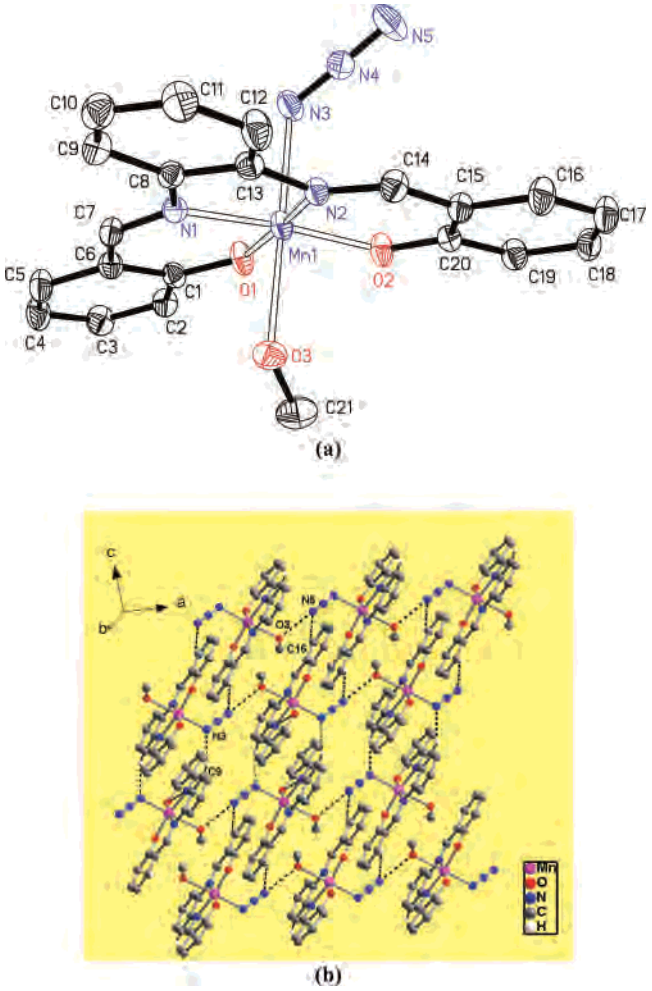

Figure 3. (a) ORTEP drawing for **3** (30% probability ellipsoids). (b) View of the two-dimensional supramolecular network of **3** linked through H bonds.

··N(5) distance of 2.774 Å, which links the mononuclear [Mn^{III}(salophen)N_3] units into an extended one-dimensional chain along the *a* axis. Furthermore, the weak hydrogen-bond interactions between carbon and nitrogen atoms lead to a two-dimensional supramolecular network in the crystal structure of complex **3** (C(16)···N(5) (2 − *x*, 2 − *y*, 2 − *z*) 3.319 Å, ∠C(16)−H···N(5) 134.3°; C(9)···N(3) (1 − *x*, 2 − *y*, 1 − *z*) 3.340 Å, ∠C(9)−H···N(3) 161.2°). The shortest intrachain and interchain Mn···Mn distances are about 7.971 and 6.818 Å, respectively, which are much longer than those in complexes **1** and **2**.

Magnetic Properties. Magnetic measurements have been carried out on crystalline samples of complexes **1**−**3**. According to the obtained data, a dominant antiferromagnetic coupling between the Mn^{III} ions in **1**−**3** can be suggested. However, in the low-temperature region they show various magnetic behaviors as discussed below.

Complex 1. The magnetic properties of complex **1** are shown in Figure 4. Figure 4a shows the temperature dependence of magnetic susceptibility from 1.9 to 300 K at a 1 kOe field. On cooling, the χ_m value increases slowly to a maximum value of 0.021 $cm^3\ mol^{-1}$ at ca. 42.0 K, and then it has a small decrease to 0.017 $cm^3 mol^{-1}$ at ca. 13.0 K, indicating the presence of an antiferromagnetic (AF)

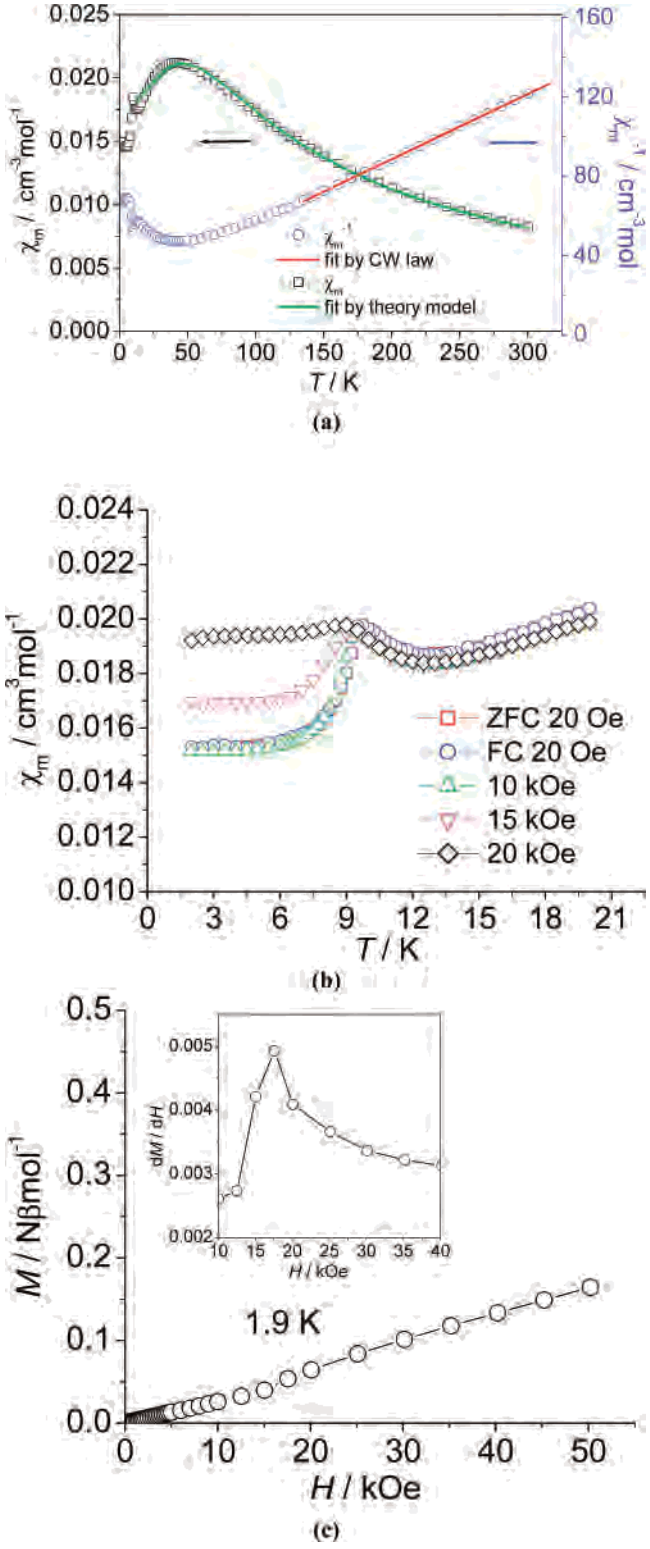

Figure 4. (a) χ_m and χ_m^{-1} vs *T* plots in an applied field of 1 kOe with a theoretical fit for **1**. (b) Zero-field-cooled magnetization (ZFC) at 20 Oe, and χ_m vs *T* plots at different fields for **1**. (c) *M* vs *H* plot at 1.9 K for **1**. The inset is the hysteresis loop for **1**.

coupling. The following little anomaly around 10.0 K may be caused by a long-range antiferromagnetic ordering, which will be proved by the subsequent magnetism measurements. With the temperature further cooling down below 10.0 K, the χ_m value shows a sharp decrease again possibly due to the effect of zero-field splitting (ZFS) arising from the Mn^{III}

ion, the antiferromagnetic interaction between chains, and/or a field saturation effect. The data above 150 K obey the Curie−Weiss law ($\chi_m = C/(T - \theta)$) with $C = 3.04$ cm^3 mol^{-1} K and $\theta = -69.7$ K. The Curie constant is close to 3.0 cm^3 mol^{-1} K as expected for one uncoupled spin-only Mn^{III} ion, while the negative θ value confirms the dominant AF coupling between Mn^{III} ions. Although this is at very low temperatures where some anisotropy may be significant, Mn^{III} is expected to be Heisenberg-like in its magnetic properties.[11] Fitting the data above 13 K using the model given by Weng and modified by Hiller[17] with $H = -2JS_{Mn}S_{Mn}$ gives the best fit parameters $J = -4.4$ cm^{-1}, $zJ' = -1.4$ cm^{-1} ($z = 4$), $g = 2.016$, and $R = 1.4 \times 10^{-4}$ {$R = \sum[(\chi_m)_{obs} - (\chi_m)_{calcd}]^2/\sum(\chi_m)_{obs}^2$} in which J and zJ' represent the intrachain and interchain coupling constants between Mn^{III} centers, respectively. These values prove an obvious AF coupling between not only intrachain Mn^{III} ions but also interchain Mn^{III} centers.

In order to further investigate the ordering phase at the low-temperature region in complex **1**, a series of $\chi_m - T$ plots in a field range of 20−20 kOe were measured. As shown in Figure 4b, there is a sharp maximum around 9.5 K in the curves below 15 kOe, which disappears at high fields (>20 kOe), indicating the occurrence of an AF ordering at low fields and a magnetic transition at high fields, probably attributed to a spin-flop process. The inflection at ca. 15 kOe in the plot of field dependence of magnetization at 1.9 K (Figure 4c) confirms the spin-flop transition induced by the exerted field, and the critical field of 17.6 kOe was determined by the dM/d$H-H$ plot (inset). Moreover, the magnetization only reaches a low value of 0.16 Nβ mol^{-1} at 50 kOe, clearly far from the expected saturation value of 4.0 Nβ mol^{-1} (for Mn^{III}, $g = 2$ and $S = 2$), which again shows the dominating antiferromagnetic coupling in **1**. The temperature dependence of the ac magnetic susceptibilities measured at different frequencies (Figure S3, Supporting Information) verifies the antiferromagnetic ordering phase transition at ca. $T_N = 9.6$ K, where the in-phase part χ_m' reaches a maximum and no obvious out-of-phase χ_m'' reflection was found.

Complex 2. The temperature dependence of the magnetic susceptibility of complex **2** was measured in 2.0−300 K with an applied field of 2 kOe, as shown in Figure 5a. On cooling, the χ_m value keeps smoothly increasing and shows a broad peak at about 30 K, which reveals an overall antiferromagnetic coupling between Mn^{III} ions in **2**. With further lowering temperature, the χ_m value exhibits an abrupt increase at around 13 K until it reaches a maximum of 0.22 cm^3 mol^{-1} at 2.0 K, attributed to the weak ferromagnetism due to spin canting. The magnetic susceptibility above 100 K can be fit to the Curie−Weiss law; the Curie constant C value of 3.05 cm^3 mol^{-1} K agrees very well with one independent high-spin Mn^{III} ion, and the negative Weiss constant θ value of −51.1 K further confirms the strong antiferromagnetic coupling in **2**. A similar method to **1** was used to deal with

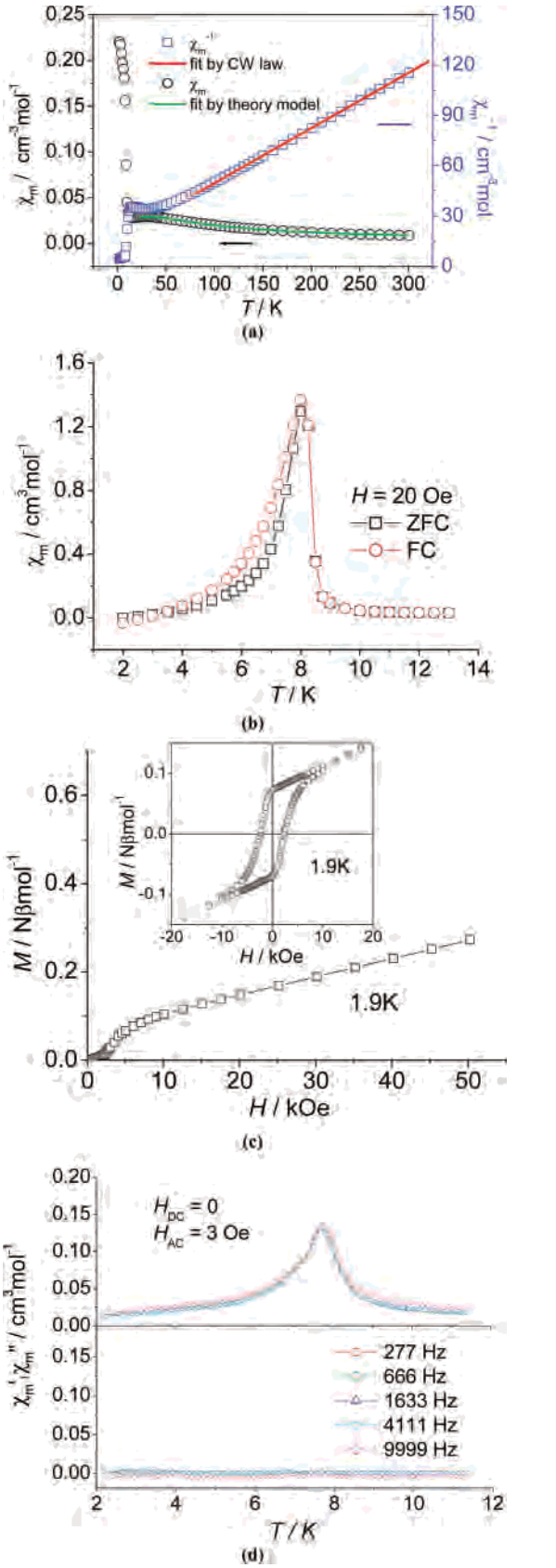

Figure 5. (a) χ_m and χ_m^{-1} vs T plots in an applied field of 2 kOe with a theoretical fit for **2**. (b) Zero-field-cooled magnetization (ZFC) and field-cooled magnetization (FC) curves at 20 Oe for **2**. (c) M vs H plot at 1.9 K for **2**. The inset is the hysteresis loop for **2**. (d) Real χ_m' and imaginary χ_m'' ac magnetic susceptibility as a function of temperature at different frequencies for **2**.

(17) (a) Weng, C. Y. Ph.D. Thesis, Carnegie Institute of Technology, **1968**. (b) Hiller, W.; Strahle, J.; Datz, A.; Hanack, M.; Hatfield, W. E.; ter Haar, L. W.; Guetlich, P. *J. Am. Chem. Soc.* **1984**, *106*, 329.

the data above 20 K with the Weng model and gives the best-fitting results: $J = -3.0$ cm^{-1}, $zJ' = -2.5$ cm^{-1} ($z = 4$), $g = 2.049$, and $R = 7.4 \times 10^{-5}$. In contrast with **1**, it seems that the intrachain coupling between Mn^{III} ions in **2** is weaker while the interchain interaction is a bit stronger.

The weak ferromagnetism of **2** was explored by measuring the zero-field-cooled (ZFC) and field-cooled (FC) magnetization at low field of 20 Oe (Figure 5b). As expected, both ZFC and FC curves show abrupt increases below 8.0 K and have a divergence, suggesting the occurrence of spin ordering. The magnetization versus field plot at 1.9 K (Figure 5c) also confirms the observed weak ferromagnetism:[18] at low field, magnetization increases steeply with magnetic field; at higher field magnetization it increases at a slower rate and in an almost linear fashion but finally only reaches ca. 0.27 Nβ mol^{-1} at 50 kOe, far from the expected saturation value of 4.0 Nβ mol^{-1} (for one Mn^{III} ion, $g = 2$ and $S = 2$). The small magnetization value at high field further proves the state of weak ferromagnetism arising from a spin canting in **2**.

Furthermore, a relatively big hysteresis loop (inset) at 1.9 K was detected in the ordered phase with a coercive field of 2.3 kOe and a remnant magnetization of 0.07 Nβ mol^{-1}. These values are more than 10 times those of the first example with $[Mn(SB)(N_3)]_n$ structure exhibiting weak ferromagnetism, $[Mn(5\text{-Brsalen})(N_3)]_n$, which has a similar structure to **1** and **2** except for the side group of SBs. The canting angle α is estimated to be about 1.0° by the expression $\sin \alpha = M_R/M_s$.[19] All the evidence discussed above suggests that complex **2** should be a weak ferromagnet caused by spin canting. However, the temperature dependence of the ac magnetic susceptibilities (Figure 5d) only exhibits the characteristic of an antiferromagnet at $T_N = 7.8$ K, where the in-phase part χ_m' reaches a maximum, while no obvious out-of-phase χ_m'' reflection was observed. Thus, we think that complex **2** may be a hidden weak ferromagnet due to spin canting.[20]

Complex 3. The magnetic property of complex **3** is relatively simple in contrast with those of **1** and **2**, as shown in Figure S4 (Supporting Information). From $\chi_m T$ versus T and χ_m^{-1} versus T plots (Figure S4a) the $\chi_m T$ value at room temperature is 3.00 cm^3 mol^{-1} K, in good accordance with the theoretical value for one spin-only high-spin Mn^{III} ion. Upon cooling, the values of $\chi_m T$ keep decreasing in the 300−1.9 K range, indicating an overall antiferromagnetic coupling in **3**. The magnetic susceptibility above 10 K can be well fit to the Curie−Weiss law with $C = 3.02$ cm^3 mol^{-1} K, $\theta = -1.9$ K. The Curie constant C value is also close to the expected value of 3.0 cm^3 mol^{-1} K for one noninteracting Mn^{III} ion ($S = 2$, $g = 2$), and the small negative θ value further confirms a possible very weak antiferromagnetic interaction in **3**. The M versus H plot measured at 2.0 K (Figure S4b) shows that magnetization increases smoothly and reaches 2.94 Nβ mol^{-1}, a bit smaller than the theoretical saturation value 4.0 Nβ mol^{-1} for one spin-only Mn^{III} ion, confirming the weak antiferromagnetic interaction between Mn^{III} ions again. Considering the long Mn···Mn distances in the structure of **3**, we fit the data in a range of 2−300 K with the spin-only susceptibility model for a single Mn^{III} ion[19] and obtained the following best results: $zJ' = -0.27$ cm^{-1}, $g = 2.028$, and $R = 6.9 \times 10^{-4}$, which also show the weak antiferromagneic interaction between the Mn^{III} ions linked through hydrogen bonds.

Similar to other azide-bridged Mn^{III} complexes,[11] these one-dimensional manganese(III) chains presented in this paper with long axial bonds should have only one dominant exchange pathway due to the small axial overlap, and it results in a weak antiferromagnetic interaction. The only magnetic orbital is the one derived from the Mn^{III} dz^2 orbital, which may make a significant contribution to the coupling. The axial ligands will mainly provide a σ-type superexchange pathway with a mechanism involving the π orbitals of the bridging group being conceived. The weak ferromagnetism in **2** should arise from the spin canting of the antiferromagnetically interacted Mn^{III} ions, and the origin of the spin canting should be mainly due to the asymmetric interactions between the neighboring Mn^{III} ions in combination with possible local anisotropy of the Mn^{III} ions.[21]

To date, with the efforts of some research groups as well as ours, a series of $[Mn(salen)(N_3)]$-type complexes has been successfully obtained by changing the substituent group of the SBs (SBs = salen, 5-Fsalen, 5-Clsalen, 5-Brsalen, and 5-OCH_3); some of their pertinent bond distances and angles and magnetic properties are listed in Table 3. We found that changing the side group of salen had little influence on the complex structures only with a subtle difference of the bond lengths and angles, which mainly consist of 1-D zigzag chains except for the special dinuclear cluster of the 5-Clsalen complex. On the other hand, they have obviously different magnetic properties at low temperatures with the change of the side group of salen, even though an overall antiferromagnetic coupling between manganese(III) ions was observed in these complexes. When salen has no side group, the corresponding complex displays no special phase transition at low temperatures, whereas when 5-Fsalen was used instead, the complex shows an antiferromagnetic ordering phase below 9.6 K. When salen was further replaced by 5-Brsalen, the combination of metamagnetism and weak ferromagnetism due to spin canting was first observed in the azide-bridged Mn^{III} complexes, and then introduction of 5-OCH_3 brought about an unprecedented hysteresis loop due to weak ferromagnetism. Noteworthy, the reported complex, $[Mn(salpn)(N_3)]_n$, has similar magnetic properties to that of $[Mn(5\text{-Fsalen})(N_3)]_n$ but different from that of $[Mn(salen)(N_3)]_n$. From Table 3 it is found that the Mn−N−N angles

(18) (a) Carlin, R. L.; Van Duyneveldt, A. J. *Magnetic properties of Transition Metal Complexes*; Springer-Verlag Inc.: New York, 1977; Vol. 2, p 184. (b) Bakalbassis, E.; Bergerat, P.; Kahn, O.; Jeannin, S.; Jeannin, Y.; Dromzee, Y.; Guillot, M. *Inorg. Chem.* **1992**, *31*, 625. (c) Sailaja, S.; Reddy, K. R.; Rajasekharan, M. V.; Hureau, C.; Rivière, E.; Cano, J.; Girerd, J.-J. *Inog. Chem.* **2003**, *42*, 180.

(19) Kahn, O. *Molecular Magnetism*; VCH: New York, 1993.

(20) (a) Engelfriet, D. W.; Groeneveld, W. L.; Groenendijk, H. A.; Smit, J. J.; Nap, G. M. *Z. Naturforsch., Teil A* **1980**, *35*, 115. (b) Tian, Y. Q.; Cai, C. X.; Ren, X. M.; Duan, C. Y.; Xu, Y.; Gao, S.; You, X. Z. *Chem. Eur. J.* **2003**, *9*, 5673.

(21) Wagner, G. R.; Friendberg, S. A. *Phys. Lett.* **1964**, *9*, 11.

Table 3. Pertinent Bond Distances (Å) and Angles (deg) for the 1-D Azide-Bridged Mn^{III}−Schiff Base Complexes **1**−**2**

	N−N	N−N−N	Mn−N	Mn−N−N	Mn···Mn* (intrachain)		T_N/K	J/cm^{-1}	ref
1 (5-Fsalen)	1.185(4)	179.8(3)	2.287(3)	114.7(2)	5.583	AF	9.6	−4.4	this work
	1.186(4)		2.327(3)	118.5(2)					
2 (5-OCH_3salen)	1.179(3)	178.3(3)	2.300(3)	116.5(2)	5.592	AF (spin canting)	7.8	−3.0	this work
	1.205(3)		2.324(3)	120.3(2)					
$[Mn^{III}(salen)(\mu_{1,3}\text{-}N_3)]_n$	1.179(3)	179.7(3)	2.280(2)	114.6(2)	5.557	AF	−	−4.5	ref 9a
	1.179(3)		2.334(2)	118.4(2)					
$[Mn^{III}(5\text{-Brsalen})(\mu_{1,3}\text{-}N_3)]_n$	1.176(4)	178.4(4)	2.299(3)	119.0(3)	5.634	AF (meta and spin canting)	6	−3.3	ref 10
	1.179(4)		2.341(3)	119.6(3)					
$[Mn^{III}(salpn)(\mu_{1,3}\text{-}N_3)]_n$	1.165(5)	178.7(4)	2.331(4)	117.3(3)	6.104	AF	below 15 K	−3.1	ref 9b
	1.190(5)		2.348(4)	137.8(3)					

in these azide-bridged Mn^{III} chains are most obviously affected by the subtle structural change, which may be one of the reasons why they possess various magnetic properties.

Conclusion

Three new Mn^{III}−Schiff base coordination complexes have been structurally and magnetically characterized in this paper. Structural analyses show that complexes **1** and **2**consist of one-dimensional azide-bridged Mn^{III} chains except for the difference of the substituent group of the auxiliary Schiff base ligand in which the N_3^- ion acts as an end-to-end bridge, while complex **3** is only a mononuclear complex with the N_3^- ion as a terminal ligand due to the change of the Schiff base ligand linked through hydrogen bonds into a two-dimensional supramolecular network. In **1** and **2** the $\mu_{1,3}$-bridging azide ion mainly mediates antiferromagnetic interaction between Mn^{III} ions compared to other similar azide-bridged Mn^{III} chains; however, **1** behaves as an antiferromagnet below 9.6 K, while **2** exhibits a hidden weak ferromagnet below 7.8 K with an unusual coercive field as large as 2.3 kOe. In comparison, **3** only displays simple weak antiferromagnetism between Mn^{III} ions. Furthermore, the successful preparation of these three complexes enriched the azide-bridged manganese(III) complexes not only structurally but magnetically.

Acknowledgment. This work was supported by the NSFC (20221101, 20490210) and National Basic Research Program of China (2006CB601102).

Supporting Information Available: CIF files of complexes **1**−**3**, plots of space packing for complexes **1** and **2**, and plots of magnetism for complexes **1** and **3**. This material is available free of charge via the Internet at http://pubs.acs.org.

IC701655W